

# QHD: A brain-inspired hyperdimensional reinforcement learning algorithm

Yang Ni<sup>1</sup>, Danny Abraham<sup>1</sup>, Mariam Issa<sup>1</sup>, Yeseong Kim<sup>2</sup>, Pietro Mercati<sup>3</sup>, and Mohsen Imani<sup>1\*</sup>

<sup>1</sup>University of California Irvine, <sup>2</sup>Daegu Gyeongbuk Institute of Science and Technology, <sup>3</sup>Intel Labs

\*Email: m.imani@uci.com

## ABSTRACT

Reinforcement Learning (RL) has opened up new opportunities to solve a wide range of complex decision-making tasks. However, modern RL algorithms, e.g., Deep Q-Learning, are based on deep neural networks, putting high computational costs when running on edge devices. In this paper, we propose QHD, a Hyperdimensional Reinforcement Learning, that mimics brain properties towards robust and real-time learning. QHD relies on a lightweight brain-inspired model to learn an optimal policy in an unknown environment. We first develop a novel mathematical foundation and encoding module that maps state-action space into high-dimensional space. We accordingly develop a hyperdimensional regression model to approximate the Q-value function. QHD-powered agent makes decisions by comparing Q-values of each possible action. We evaluate the effect of the different RL training batch sizes and local memory capacity on the QHD quality of learning. Our QHD is also capable of online learning with tiny local memory capacity, which can be as small as the training batch size. QHD provides real-time learning by further decreasing the memory capacity and the batch size. This makes QHD suitable for highly-efficient reinforcement learning in the edge environment, where it is crucial to support online and real-time learning. Our solution also supports small experience replay batch size that provides 12.3× speedup compared to DQN while ensuring minimal quality loss. Our evaluation shows QHD capability for real-time learning, providing 34.6× speedup and significantly better quality of learning than state-of-the-art deep RL algorithms.

## 1 INTRODUCTION

Reinforcement Learning (RL) has opened up new opportunities to solve a wide range of complex predictions and decision-making tasks that were previously out of reach for a machine [1, 2]. Compared to supervised and unsupervised learning methods, RL does not have direct access to labeled training data. Instead, it trains a self-learning agent using the observations of states and feedback rewards from the environment [3]. The learning process of RL is similar to how human beings learn to perform a new task. Initially, the RL agent interacts with the environment and tries to take action with no prior knowledge or past experience. Learning through the interaction of an environment makes RL appealing to the field of dynamic control and automated system optimization, where the optimal policy is hard to define and is constantly changing with its environment [1].

Q-learning is one of the most popular model-free reinforcement learning methods. With the advancement in Deep Neural Networks (DNNs), the traditional Q-learning methods are changing to Deep

Q-Networks (DQN) [4]. Unlike Q-learning that relies on large tables, DQN exploits DNN to learn an approximation of Q-value for every pair of action and state. In DQN, the actions and states are inputs to a DNN and the outputs are Q-values for each possible action. Recently, there has been active developments for various DQN applications such as playing GO [5] and computer games [6], system optimization [7], Genomics [8–10], and dynamic resource management [11]. DQN is capable of learning complex tasks without modeling the environment, but its power comes at a price, i.e., the huge computation cost and long learning time. This makes it only suitable for powerful computers in the cloud rather than mobile devices at the edge. However, edge devices play an increasingly important role in daily life, and they directly interact with the environment and collect feedback. Edge devices are natural platforms for RL, except that they have a limited energy budget and computation power. Offloading RL to the cloud not only leads to extra communication overhead but also causes security and privacy concerns.

To apply RL at the edge for mobile and sensor-like devices, we redesign the RL algorithm by exploiting the brain-inspired Hyperdimensional Computing (HDC) [12]. Compared to DNN, HDC is highly efficient and robust against noise. HDC is motivated by how human brains process different kinds of inputs, i.e., brains express information using a vast number of neurons. The information is then processed and memorized in a holistic and high-dimensional way. HDC is powered by a set of well-defined HDC operations that mimic the functionalities of human brains and enable learning. For inputs in the lower-dimensional space, HDC usually encodes them to vectors of several thousand dimensions, i.e., hypervectors. The learning process is based on highly-parallelizable operations of hypervectors, such as element-wise addition and multiplication. Thus, HDC has been applied as a lightweight machine learning solution to multiple applications, e.g., bio-signal classification [13, 14], speech recognition [15], reasoning [16, 17]. In these applications, HDC is capable of achieving comparable accuracy to DNN with significantly higher efficiency. HDC also possesses an intriguing beneficial advantage from its brain-like memorization ability, i.e., HDC achieves one-shot or few-shot learning with high quality [18].

However, current HDC solutions mainly focus on traditional classification and clustering. In contrast, in this paper, we propose QHD, a Hyperdimensional Reinforcement Learning, that mimics brain properties towards robust and real-time learning. The main contributions of the paper are listed as follows:

- To the best of our knowledge, QHD is the first hyperdimensional reinforcement learning algorithm. QHD relies on lightweight HDC models to learn an optimal policy in an unknown environment. We first develop a novel mathematical foundation

and encoding module that maps state-action space into high-dimensional space. We accordingly develop a hyperdimensional regression model to approximate the Q-value function. QHD-powered agent makes decisions by comparing Q-values of each possible action. Our neural-inspired QHD uses operations that are extremely hardware-friendly for edge devices.

- We evaluate the effect of the different RL training batch sizes and local memory capacity on the QHD quality of learning. Thanks to the brain-like hyperdimensional operations, QHD is able to utilize even a small amount of available training data. It thereby supports a much smaller training batch size than DQN while still providing high-quality results. Our QHD is also capable of online learning with tiny local memory capacity, which can be as small as the training batch size. QHD provides real-time learning by further decreasing the memory capacity and the batch size. This makes QHD suitable for highly-efficient reinforcement learning in the edge environment, where it is crucial to support online and real-time learning.

We compare our QHD accuracy and efficiency with the state-of-the-art DQN algorithms for multiple dynamic control tasks. Our evaluation shows that QHD achieves significantly better overall efficiency than DQN while providing higher or comparable rewards. Our solution also supports a small experience replay batch size that provides 12.3× speedup compared to DQN while ensuring minimal quality loss. Our evaluation shows QHD capability for real-time learning, providing 34.6× speedup and significantly better quality of learning than state-of-the-art deep RL algorithms.

## 2 RELATED WORK

**Reinforcement Learning:** In recent years, reinforcement learning algorithms have obtained dramatically more attention from researchers because of the advancement in Deep Reinforcement Learning (DRL). DRL is capable of dealing with complicated action-environment interactions and large action/state spaces. DRL algorithms such as DQN greatly expand the application of RL to fields like computer games [6, 19], transportation optimization [20, 21], network optimization [22, 23] and health care [24, 25]. In [21], researchers focus on the driver dispatch optimization within the online ride-sharing services, which is becoming essential for the public transportation of big cities. They use DQN to learn a policy for matching available drivers and users in order to maximize the success rate while minimizing the wait time. In the biomedical field, DRL contributes to an automated radiation adaptation protocol for radiotherapy of lung cancer patients [24]. All works mentioned above utilize DNN to handle complex agent-environment interaction. However, the frequent DNN model update during RL training process is computationally intensive and thus not suitable for learning at the edge. In contrast, we propose a brain-inspired reinforcement learning solution with inherent efficiency and robustness. Comparing to existing deep RL solutions, our method focuses on better energy efficiency during the learning process while maintaining high-quality results.

**Hyperdimensional Computing:** Hyperdimensional Computing is a brain-like computational model and an alternative lightweight

machine learning algorithm. Prior HDC works mainly provide solutions to classification and cognitive tasks, such as bio-signal processing [13, 14], speech recognition [15, 18], robotic control [26] and multi-sensor signal classification [27]. Work in [14] uses a HDC-based method for electroencephalography (EEG) error-related signal classification. HDC provides comparable learning accuracy to traditional machine learning methods while ensuring higher computational efficiency. In these highlighted machine learning applications, HDC has outperformed state-of-the-art machine learning solutions, e.g., support vector machines [18, 28] and neural networks [26, 27, 29, 30]. Unlike all prior works, this paper is the first effort focusing on HDC-based reinforcement learning. We develop a novel algorithm to train a self-learning agent to better interact and learn the environments. Our solution significantly improves the computational efficiency and robustness as compared to existing deep RL techniques.

## 3 QHD: HYPERDIMENSIONAL Q-LEARNING

### 3.1 Overview

Figure 1 shows an overview of QHD supporting hyperdimensional reinforcement learning. In our RL task, there are two components (Agent and Environment) and three variables (Action, State and Reward). Figure 1(a) exploits a Cartpole example to illustrate these components and variables. The cartpole is the agent, and the space around it is the environment. The cart either goes right or left, which forms the action space of the agent. The position and velocity of the cart as well as the pole angle and angular velocity, form a state vector at each time step. For each step, the cart chooses an action, then the state of the cart and pole will be updated accordingly. Depending on the pole being balanced or not, the cart gets either a positive reward or a zero reward as the feedback from the environment. As shown in Figure 1, the interaction between the agent and environment form a loop in which the action taken based on the current state leads to the next state and reward. On the other hand, we have a trajectory composed of different states, rewards, and actions from each time step until the pole loses balance. The trajectory of each episode is saved in local memory for later learning. In Figure 1(b), we provide an overview of QHD algorithm guiding the agent in the decision-making process. In each time step, we map the state vector to a holographic hypervector using the HDC encoder. The hyperdimensional regression algorithm then predicts the Q-value for each possible action based on the input state hypervector. The final step of QHD chooses an action with the highest Q-value. In the remaining parts of this section, we introduce the HDC encoder, HDC regression, and the training of the QHD.

### 3.2 QHD Hyperdimensional Encoding

In QHD algorithm, the learning process starts by mapping the current state vector from the original to high-dimensional space, i.e., hypervector encoding. One characteristic of this high-dimensional space is that we can create a large number of nearly orthogonal hypervectors through random sampling. Unlike the original HDC encoder that operates over binary or bipolar representation, our solution generates hypervectors with random exponential elements, e.g.,  $\vec{H}_1$  belongs to  $\{e^{i\theta} : \theta \in [-\pi, \pi]\}^D$ .

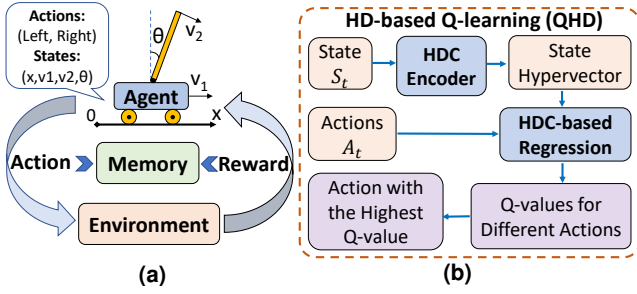


Figure 1: Overview of QHD reinforcement learning.

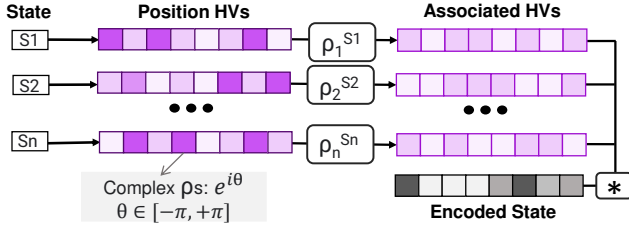


Figure 2: Hyperdimensional encoding with complex bases.

For example, if we create two randomly generated hypervectors,  $\vec{H}_1$  and  $\vec{H}_2$ , then we have the cosine similarity  $\delta(\vec{H}_1, \vec{H}_2) = (\vec{H}_1 \cdot \vec{H}_2) / (|\vec{H}_1| |\vec{H}_2|) \approx 0$ . This allows the HDC encoder to express the input using a holographic hypervector through well-defined hypervector operations. In other words, the original information is evenly distributed across all hypervector elements. The advantage of holographic representation is that we can accumulate information by combining two hypervectors, which is also reversible. Next, assuming the same two random hypervectors  $\vec{H}_1, \vec{H}_2$  as above, we define the following HDC mathematics to model brain functionalities:

**Bundling:** This operation stands for component-wise addition of hypervectors. Bundling operation is the core of memorization for HDC models, in which the information from multiple hypervectors is saved into one single hypervector. The bundled hypervector is similar to every component hypervector, i.e.,  $\delta(\vec{H}_1 + \vec{H}_2, \vec{H}_1) \gg 0$ . Thus, we represent sets using bundling operation.

**Continuous Binding:** The goal of binding is to associate items in hyperspace. Figure 2 shows the functionality of our continuous binding. Assuming we have an  $n$ -element state vector  $S_t = \{s_1, s_2, \dots, s_n\}$  at time step  $t$ . For tasks with continuous state, we have  $S \in \mathcal{R}^n$ .

Our encoding generates a random exponential hypervector for each feature position  $\{\vec{P}_1, \vec{P}_2, \dots, \vec{P}_n\}$  and then performs encoding as:

$$\vec{H}_1 = \vec{P}_1^{s_1} * \vec{P}_2^{s_2} * \dots * \vec{P}_n^{s_n}$$

We define  $\vec{P}_k^{s_k}$  to be the component-wise exponential of  $\vec{P}_k$ . Bundling of several encoded states results in generating a memory hypervector:  $\vec{R} = \vec{H}_1 + \vec{H}_2 + \dots + \vec{H}_m$ . Our solution is extremely flexible to move, rotate, or decode any state in high-dimension space. For example, an encoded state can be moved by  $\Delta s$  to left by binding the high-dimensional representation to  $\vec{P}_k^{-\Delta s}$ . In other

words,  $\vec{H} * \vec{P}_1^{-\Delta s} = \vec{P}_1^{(s_1 - \Delta s)} * \dots * \vec{P}_n^{s_n}$ . We exploit this adaptive and flexible representation to also decode an object from high-dimension. For instance, we can extract  $s_1$  value by exploring  $\Delta s$  value until  $s_1 - \Delta s = 0$ , therefore,  $\vec{P}_1^{(s_1 - \Delta s)} = \vec{P}_1^0 = 1$ . This can be detected by looking at the similarity of shifted vectors with the original encoded data. Another advantage of our mathematics is its capability to decode or extract information independent of the number of features. As a result, our solution can explore the space, decode information from desired features, and potentially provide analogy and reasoning.

To improve the existing HDC encoding, we introduce the idea of a continuous complex vector method. The idea is to generate a position hypervector,  $\vec{P}$ , for each position/feature, which is correlated based on the distance between them. That is, the  $\vec{P}$ s that represent nearby locations should be similar to each other, and the  $\vec{P}$ s which represent far locations, should have almost orthogonal distribution:  $\delta(\vec{P}^x, \vec{P}^y) = \sum_i e^{i\theta_i(y-x)} \approx \mathbb{E}(e^{i\theta(y-x)})_{p(\omega)} = k(x-y)$ , where,  $k(x-y)$  is a shift-invariant kernel, which is the Fourier transform of the probability distribution.

To evaluate the similarity for Norm encoding, we first consider the hypervectors  $\rho^x * \vec{R}_1$  and  $\rho^y * \vec{R}_2$ , since they form the building blocks of all our encoding. Their similarity is given by

$$\delta(\vec{P}^x * \vec{R}_1, \vec{P}^y * \vec{R}_2) \approx \mathbb{E}(\vec{P}_i^{y-x} \vec{R}_{1,i}^\dagger \vec{R}_{2,i}) \approx \delta(\vec{P}^x, \vec{P}^y) \delta(\vec{R}_1, \vec{R}_2)$$

The error in this approximation will be due to random covariances, which will tend to 0 as we increase the dimension  $D$  (which corresponds to the number of samples while taking the expectation values). Since both these similarities are real, we need to consider only their real parts. First term  $\delta(\vec{R}_1, \vec{R}_2)$  can be written as  $\frac{1}{D} \sum_{i=1}^D \cos(\alpha_i - \beta_i)$ , where  $\alpha_i$  and  $\beta_i$  are uniformly sampled from  $[-\pi, \pi]$ . If  $\vec{R}_1 = \vec{R}_2$ , then this similarity is 1. Otherwise, because the angles matter only modulo  $2\pi$ , we can consider  $\alpha_i - \beta_i$  to be randomly sampled from  $[-\pi, \pi]$ . Assuming that  $D$  is large, we have:  $\delta(\vec{P}^x, \vec{P}^y) \sim N(k(x-y), \frac{\sigma_{p(\omega)}}{\sqrt{D}})$ .

### 3.3 QHD Hyperdimensional Regression

We develop a regression model based on hyperdimensional mathematics. Recall Figure 1(b), the input to our hyperdimensional regression model is the action for evaluation and the encoded state hypervector. The output is the action-state value or Q-value corresponding to the input. Our regression consists of multiple model hypervectors  $\{\vec{M}_1, \vec{M}_2, \dots, \vec{M}_n\}$ , where  $n$  is the size of the action space. For evaluation of each action at time step  $t$ , we only select one of the model hypervectors  $\vec{M}_A$  that corresponds to a certain action  $A$ , and the regression is operated on the current-step state hypervector  $\vec{S}_t$ . These model hypervectors are initialized to all zero elements and have the same dimensionality as the encoded state hypervector, i.e.,  $\vec{M}_A \in \{0\}^D$ . Even though RL is not a typical supervised learning task, the regression part of it trains under supervision. In the context of QHD, the true value is given by the ideal Q-function, and we use hyperdimensional regression to approximately calculate the Q-value. We explain the ground truth for Q-value in Section 3.4 when we introduce QHD. On the other hand, the approximated Q-value for action  $A$  is given through the dot product between the model hypervector and the encoded state

hypervector:  $q_{pred} = \vec{M}_A \cdot \vec{S}^T$ , where  $\vec{S}^T$  is a conjugate of the encoded query with complex elements. As for the regression model update, we use the error between  $q_{pred}$  and  $q_{true}$  (ground truth). We either add or subtract a portion of the state hypervector to the model, weighted by the regression error.

$$\vec{M}_A = \vec{M}_A + \beta(q_{true} - q_{pred}) \times \vec{S}$$

This equation ensures that the model gets updated more aggressively for higher prediction error rates ( $q_{true} - q_{pred} \gg 0$ ). In order to have a smooth training process, we control the model update speed by multiplying a learning rate  $\beta$ . Thus, we gradually update the regression model with iterative training, and the approximation of Q-values becomes more accurate. The lightweight operations in our regression design, such as component-wise addition, contribute to the fast learning process for QHD.

### 3.4 Hyperdimensional Value-based Reinforcement Learning

In this section, we present the details for our QHD, a hyperdimensional Q-learning algorithm. We start our introduction with how agents with QHD make decisions at each time step. Current Q-learning methods, such as DQN, are value-based RL, meaning they do not directly learn a policy. Instead, they apply an indirect policy backed by the value function. In QHD, we use a greedy policy that prefers actions with higher Q-values. However, it is crucial to balance the exploration of the environment and the exploitation of the learned model. For example, always selecting actions with the highest Q-value will easily result in a sub-optimal result that gets stuck in a local minimum. This is because agents have not explored enough, and their decisions are short-sighted. On the other hand, if agents spend too much time trying new actions instead of following the learned model, we again have lower quality results. Therefore, we combine a random exploration strategy with the greedy policy, i.e.,  $\epsilon$ -decay policy. Assuming the action space  $\mathcal{A}$  and time step  $t$ :

$$A_t = \begin{cases} \text{random action } A \in \mathcal{A}, & \text{with probability } \epsilon \\ \text{argmax}_{A \in \mathcal{A}} Q(S_t, A), & \text{with probability } 1 - \epsilon \end{cases}$$

The probability of selecting random actions will gradually drop after the agent explores and learns for several episodes. In experiments, we use a rate of changing  $\epsilon$ -decay less than 1; this ensures that QHD agents start to trust their learned model more and lessen the importance of exploration. In the equation above,  $Q(S_t, A)$  is a hyperdimensional regression model that returns approximated Q-values for input action-state pairs. Once an action  $A_t$  is chosen by QHD, the agent interacts with the environment. We then obtain the new state  $S_{t+1}$  for the agent and the feedback reward  $R_t$  from the environment. At the next time step  $t + 1$ , QHD selects another action  $A_{t+1}$  according to the  $\epsilon$ -decay policy based on the updated state. This chain of actions and feedbacks form a trajectory or an episode until some termination conditions are met. To train an RL algorithm, these episodes or past experiences are usually saved to local memory as training samples. More specifically, we save a tuple of four elements for each step:  $(S_t, A_t, R_t, S_{t+1})$ .

In DQN, the RL training process and parameter update are based on DNN back-propagation, while the training in QHD utilizes more efficient hypervector operations. The regression model in QHD is trained at the end of each time step after saving current information

---

#### Algorithm 1 QHD: HDC-based Reinforcement Learning

---

**for** Episode  $i$  **do**

**for** Time step  $t$  **do**

    Get current state vector  $S_t$

$\epsilon$ -greedy algorithm for choosing action  $A_t$

    Get reward  $R_t$  and new state  $S_{t+1}$

    Record  $\{S_t, A_t, R_t, S_{t+1}\}$  to memory

    Call function **TrainQHD** for QHD training

  Exploration rate decays

**if** After  $\tau$  episodes **then**

    Copy QHD model  $Q$  to delayed QHD model  $Q'$

**function** **TRAINQHD**

  Sample an experience batch  $E$  from memory

**for**  $\{S_t, A_t, R_t, S_{t+1}\}$  in  $E$  **do**

    Calculate predicted q-value  $q_{t\_pred}$  using (1)

    Calculate true q-value  $q_{t\_true}$  using (2)

    Update hyperdimensional regression model  $Q$  with (3)

---

to the local memory. As in the DQN training process, we apply a strategy called experience replay. Unlike offline supervised learning, where the training dataset is fixed, it is common to have a stream of training samples in RL. Thus, it is important to refresh the memory of past learning experiences while processing the new inputs. However, in ideal settings, i.e., the capacity of local memory is unlimited, the number of training samples grows so large in the end that it becomes time-consuming to train on the full dataset. Thus, the experience replays in QHD samples a training batch from the local memory and uses it for the regression model update. The training batch includes multiple tuples of past experiences.

Now assume we sample a one-step experience tuple from past trajectories to train our QHD, i.e.,  $(S_t, A_t, R_t, S_{t+1})$ . In Section 3.3, we introduce the regression model update based on the approximation error. We first encode the input state  $S_t$  to the hypervector  $\vec{S}_t$  and the predicted value  $q_{t\_pred}$  is simply calculated as:

$$q_{t\_pred} = Q(S_t, A_t) = \vec{S}_t^T \cdot \vec{M}_{A_t} \quad (1)$$

For supervised regression training, we need a ground truth  $q_{t\_true}$ . We cannot directly obtain the true Q-value because RL is not typical supervised learning. For time step  $t$ , the feedback is the one-step reward  $R_t$  while the Q-value is the expectation of accumulated rewards. The method to connect these two values is called the Bellman Equation or Dynamic Programming Equation [31]. Since most RL tasks can be viewed as a Markov Decision Process (MDP), the Bellman equation gives a recursive expression for the Q-value at step  $t$ , the expected sum of current rewards, and the Q-value for step  $t + 1$ . To learn an optimal Q-function, we use the Bellman optimality equation as shown below:

$$q_{t\_true} = R_t + \gamma \max_{A'} Q'(S_{t+1}, A) \quad (2)$$

Recall that our objective in QHD is to achieve optimal policy and maximize the accumulated rewards within one episode. The Bellman optimality equation states that, in order to achieve optimal results for the whole task, we need to optimize each sub-task. Thus, the true value  $q_{t\_true}$  is the sum of  $R_t$  and the max next-step Q-value. Instead of using model  $Q$  to calculate the maximum

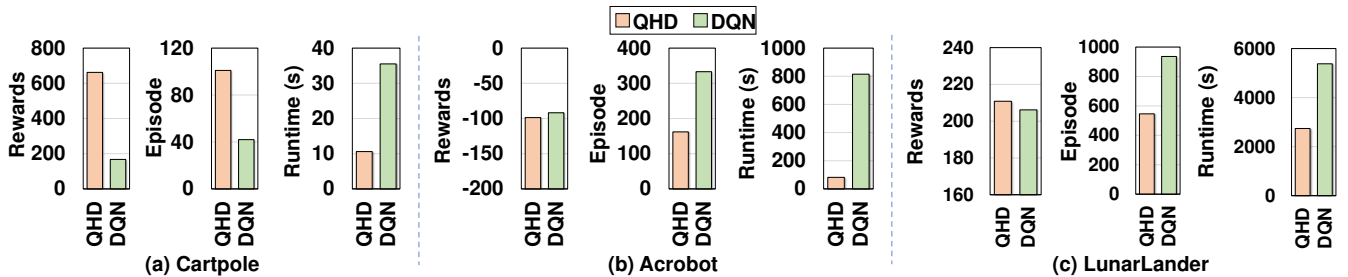


**Figure 3: Performance comparison between DQN and QHD:** In (a), the Cartpole reward is averaged over the last 50 episodes; the number of episodes and runtime are recorded when the episodic reward surpasses 200. In (b), the Acrobot reward is averaged over the last 100 episodes; the rest is recorded when the past-100-episode average reward reaches -120. In (c), the LunarLander reward is averaged over the last 100 episodes; the rest is recorded when the past-100-episode average reward reaches 200.

next-step Q-value, we use a delayed model  $Q'$  which gets updated periodically using parameters in  $Q$ . This method is called Double Q-learning [32]; it stabilizes the learning process and avoids the overestimation of Q-value caused by the maximization in the Bellman equation. We also include a reward decay term  $\gamma$  that adjusts the effect of future rewards on the current step Q-value. If  $\gamma$  is close to 1, QHD takes more long-term effects into consideration, while when  $\gamma$  is close to 0, the model considers mostly the effect of immediate rewards and thus being short-sighted. It is worth noting that a smaller  $\gamma$  is not necessarily bad because some tasks do not have a long-term effect.

After obtaining the predicted Q-value and true Q-value, we perform regression model update. We update the model corresponding to the action taken, using the regression error  $q_{t\_true} - q_{t\_pred}$  and the encoded state hypervector. The learning rate is  $\beta$ .

$$\vec{M}_{A_t} = \vec{M}_{A_t} + \beta(q_{t\_true} - q_{t\_pred}) \times \vec{S}_t \quad (3)$$

In Algorithm 1, we conclude how QHD learns in an episodic RL environment using the equations and procedures introduced above.

## 4 EXPERIMENTAL RESULT

### 4.1 Experiment Settings

We implement our QHD algorithm on CPU hardware platform Intel Core-i7 10700 using Python. We validate the functionality of QHD with multiple control tasks in the OpenAI Gym [19] and a resource management task. For the control tasks, we selected Cartpole, Acrobot and LunarLander. The objective of Cartpole is to keep the balance of an uprising pole that loosely connects to a moving cart. Acrobot is a system with two links and two joints, where force is applied to the joint between the two links. The objective of Acrobot is to swing the lower part of the hanging link until it reaches the target height. The target in the LunarLander task is to safely land the moon vehicle on the uneven ground as fast as possible by controlling three engines. For comparison, we use the DQN algorithm for the same tasks in our evaluation. In the following subsections, we compare these two methods' learning performance and efficiency in all tasks. We run both methods for 200 episodes for the Cartpole task, 500 episodes for Acrobot and 1000 episodes for LunarLander. The maximum number of steps for each episode is 1000 for Cartpole/LunarLander and 500 for Acrobot.

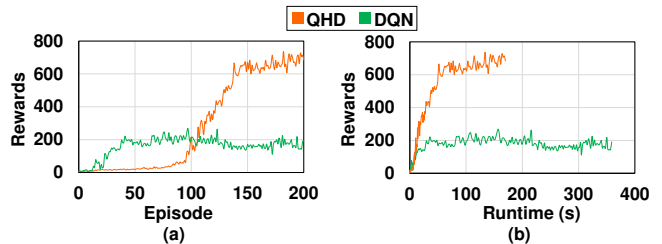


**Figure 4: QHD and DQN Cartpole rewards comparison:** In (a), average rewards trajectory is plot with episode index; (b) presents the trajectory with runtime as x-axis.

The regression model we used in QHD has dimensionality  $\mathcal{D} = 6000$  unless stated otherwise. The DQN is powered by a neural network with two hidden layers. The first layer has 128 neurons, and the second one has 256; except in the LunarLander task, where we use 64 neurons for the first layer and 128 for the second layer. The experience replay is enabled for model training in both methods, and we assume unlimited memory for rewards and runtime comparison. We select different parameters for sampling training batches to ensure the best learning quality for both methods. The QHD training batch size is 4 for Acrobot/Cartpole and 10 for LunarLander, and the DQN training batch size is 64 for all tasks. Rewards and runtime results for both methods are averaged over multiple trials.

### 4.2 RL Rewards & Runtime comparison

Figure 3 compares the performance of DQN and QHD over three popular OpenAI control tasks. The bar graphs compare the final rewards achieved by both methods and the runtime needed for reaching preset goals. We set the goal of Cartpole as keeping balance for more than 200 steps, i.e., the episodic reward is larger than 200. As for Acrobot, the goal is to reach the target height within 120 steps, which means the reward is larger than -120. The goal in LunarLander task is 200 rewards. In this figure, we use slightly different criteria for achieving goals in three tasks. For Cartpole, we focus on the immediate episodic reward in runtime comparison because the DQN method cannot stabilize above 200 rewards. For Acrobot and LunarLander, we collect the average reward over the

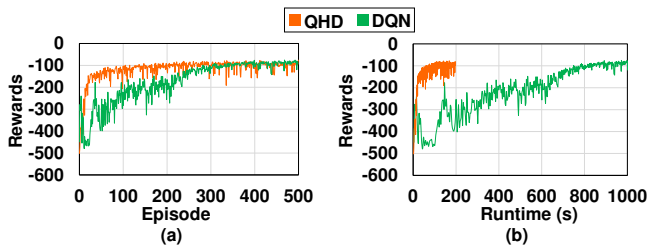


Figure 5: QHD and DQN Acrobot rewards comparison with both episode index and runtime index.

past 100 episodes as the standard. As shown in Figure 3(a) and 4, QHD achieves significantly higher final rewards in Cartpole compared to DQN. Within 200 episodes, QHD provides an averaged episodic reward over 660, which is nearly  $4\times$  higher than DQN. Note that QHD may need a higher number of episodes than DQN. For example, QHD reaches 200 rewards after 101 episodes while DQN only needs 42 episodes. However, considering the total execution time (shown in Figure 4b), QHD is significantly faster than DQN. This efficiency comes from the lightweight nature of QHD.

We also present the result comparison for the Acrobot task in Figure 3(b) and 5. As for the quality of learning, QHD achieves similar results compared to DQN. The averaged reward of QHD is slightly lower than that of DQN due to fluctuation at the end of the trial. However, our QHD provides significantly better learning efficiency compared to DQN. QHD is about  $10\times$  faster than DQN in terms of runtime and uses  $2\times$  fewer number of episodes. In the figure, we show that our QHD converges to the goal much faster at the beginning of the learning process. The ability of QHD to rapidly capture patterns in the environment and accurately memorize past experience is very appealing to RL tasks.

As for the LunarLander task, we compare the RL performance and runtime in Figure 3. It shows that, comparing to DQN, our QHD provides significantly higher efficiency in terms of both number of episodes and actual runtime while also achieving slightly higher rewards. QHD achieves the goal nearly 400 episodes earlier than DQN and about 2600 seconds (2 times) faster in runtime.

### 4.3 Evaluate the effect of training batch size

As we mentioned in 3.4, both our QHD and DQN relies on experience replay that periodically provides the learning agent with the past experience. Since the memory is assumed to be infinite and the reinforcement learning process can be extended to infinite episodes, we need to sample the training dataset from the large memory with preset batch size. This parameter is rather crucial because it controls how much past experience is available for the agent to learn from, thereby deeply influencing the learning quality. Usually, a larger batch size provides the agent with a better view of the environment and prevents it from forgetting past experience. However, increasing the number of training samples also brings greater computation and communication costs, which is not ideal for efficient learning at the edge. Our QHD, on the other hand, aims to fully utilize the provided training samples at each step; and we observe from the following results that it relieves the requirement for large batch sizes and saves the runtime for RL training.

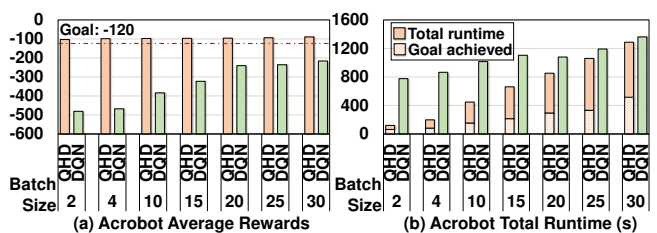


Figure 6: Explore the effect of batch size on both DQN and QHD using Acrobot task: In (a), we record average rewards of the last 100 episodes. In (b), we record the total runtime for 500 episodes and collect the goal-achieved runtime when QHD reaches the average reward of -120.

In Figure 6, we explore the effect of replay batch size on both methods using the Acrobot task. Figure 6a compares the average rewards for the last 100 episodes, and it is clear that our QHD performs significantly better than DQN for different batch size settings, especially for smaller batch sizes. For example, when we only provide two random samples for each model training step, QHD can still achieve the goal with an average of -102.9 rewards. On the other hand, DQN performs poorly with the reward of -480.9, which is close to the lowest possible reward of -500. This means that DQN fails to learn the Acrobot task, and it does not efficiently utilize the limited available training samples. We also observe that increasing the batch size by a large amount from 2 to 30 helps DQN achieve better average rewards of -215.9. However, it is still unable to reach the goal of -120 rewards even with  $15\times$  larger batch size than the minimum setting of QHD. When we increase the batch size for QHD, the figure shows a steady increase in average rewards. When the batch size of QHD is set to 30, it achieves higher rewards than the DQN results shown in the last section with a batch of 64.

Apart from better performance, our QHD also provides higher efficiency. In Figure 6(b), We compare the total runtime of QHD and DQN with different batch sizes. For QHD, we provide both the runtime for 500 episodes and the runtime when the goal is achieved. For DQN, only total runtime is provided because DQN cannot achieve the goal with small batch sizes from 2 to 30. Our QHD is constantly faster than DQN for these batch size settings. With the batch size of 2 (15), our QHD is about  $6.5\times$  ( $1.7\times$ ) faster than DQN in terms of total runtime. Focusing on the actual runtime when achieving the target, QHD shows an even larger improvement, e.g., the speedup is about  $12.3\times$  ( $2.6\times$ ) with the batch size of 2 (30).

### 4.4 QHD vs. DQN with Limited Memory

In the above sections, we assume the local memory for RL experience replay has infinite capacity, i.e., the agent has access to all previous experience during the training. Even though we use sampling to select training sets, each data point in memory can possibly be used for training. However, in practical implementations of RL algorithms, the memory capacity is limited due to energy and space budgets, especially in the low-power edge environment. Thus, in this section, we evaluate the performance of our QHD with limited memory size and compare it to the DQN results.

In Figure 7(a), we present the average reward achieved by both methods under different memory capacity limitations. The reward

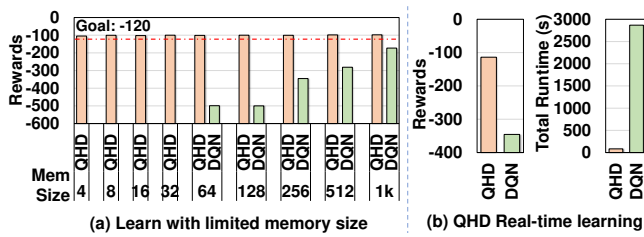


**Figure 7: QHD learning efficient with tiny local memory.** is averaged over the last 100 episodes. When collecting these results, we fix the training batch size; the batch size is 4 for QHD and 64 for DQN. We vary the memory size from 1 to 1024 for QHD, and the minimum memory size setting for DQN is 64 because of its higher requirement on training batch size. The figure shows that DQN performs poorly when the memory size is 64 and 128, with an average reward of  $-500$ . When we increase the memory size to at least 256, i.e.,  $4\times$  of the batch size, DQN starts to learn but ends without reaching the  $-120$  target. However, our QHD can reach that goal even with a memory size as large as its batch size. These results show that QHD can perform RL tasks with online learning, i.e., a tiny local memory.

We also take one step further to explore the QHD capability of real-time learning. We set both the batch and memory sizes to 1, which means the agent will learn based on only the current sample, without any access to previous experiences. To handle this real-time learning setting, the RL algorithm should have the ability to fully memorize the current sample and efficiently utilize this one-time training data point. We use DQN with 256 memory size and 64 batch size as an online-learning comparison since DQN does not learn with a real-time setting. As shown in Figure 7(b), even with larger memory size and batch size, DQN achieves significantly lower rewards ( $-345.4$ ). For a 500-episode training, our QHD achieves average rewards of  $-113.7$  using 83 seconds, which leads to a  $34.6\times$  speedup in total runtime.

## 5 CONCLUSION

We propose a novel lightweight RL algorithm based on brain-inspired hyperdimensional computing. QHD utilizes hardware-friendly hyperdimensional operations for high-quality Q-value approximation and self-learning agent training. Our evaluation on several control tasks shows that QHD provides significantly higher efficiency and better learning quality than existing DQN approaches. Our solution also supports small experience replay batch sizes that provide  $12.3\times$  speedup compared to DQN while ensuring minimal quality loss.

## ACKNOWLEDGEMENTS

This work was supported in part by National Science Foundation #2127780, Semiconductor Research Corporation (SRC) Task #2988.001, Department of the Navy, Office of Naval Research, grant #N00014-21-1-2225 and #N00014-22-1-2067, Air Force Office of Scientific Research, grant #FA9550-22-1-0253, and a generous gift from Cisco.

## REFERENCES

[1] M. Botvinick, S. Ritter, J. X. Wang, Z. Kurth-Nelson, C. Blundell, and D. Hassabis, "Reinforcement learning, fast and slow," *Trends in cognitive sciences*, vol. 23, no. 5,

pp. 408–422, 2019.

[2] P. Henderson *et al.*, "Deep reinforcement learning that matters," in *Proceedings of the AAAI conference on artificial intelligence*, 2018.

[3] V. François-Lavet *et al.*, "An introduction to deep reinforcement learning," *arXiv preprint arXiv:1811.12560*, 2018.

[4] T. Hester *et al.*, "Deep q-learning from demonstrations," in *Thirty-second AAAI conference on artificial intelligence*, 2018.

[5] D. Silver *et al.*, "Mastering the game of go with deep neural networks and tree search," *nature*, vol. 529, no. 7587, pp. 484–489, 2016.

[6] V. Mnih *et al.*, "Playing atari with deep reinforcement learning," *arXiv preprint arXiv:1312.5602*, 2013.

[7] N. Jay *et al.*, "A deep reinforcement learning perspective on internet congestion control," in *International Conference on Machine Learning*, PMLR, 2019.

[8] M. Imani *et al.*, "Partially-observed discrete dynamical systems," in *2021 American Control Conference (ACC)*, pp. 310–315, IEEE, 2021.

[9] M. Imani *et al.*, "Scalable inverse reinforcement learning through multifidelity bayesian optimization," *IEEE transactions on neural networks and learning systems*, 2021.

[10] M. Imani *et al.*, "Control of gene regulatory networks using bayesian inverse reinforcement learning," *IEEE/ACM transactions on computational biology and bioinformatics*, vol. 16, no. 4, pp. 1250–1261, 2018.

[11] Y. He *et al.*, "Software-defined networks with mobile edge computing and caching for smart cities: A big data deep reinforcement learning approach," *IEEE Communications Magazine*, vol. 55, no. 12, pp. 31–37, 2017.

[12] P. Kanerva, "Hyperdimensional computing: An introduction to computing in distributed representation with high-dimensional random vectors," *Cognitive computation*, vol. 1, no. 2, pp. 139–159, 2009.

[13] A. Moin *et al.*, "A wearable biosensing system with in-sensor adaptive machine learning for hand gesture recognition," *Nature Electronics*, 2021.

[14] A. Rahimi *et al.*, "Hyperdimensional computing for blind and one-shot classification of eeg error-related potentials," *Mobile Networks and Applications*, vol. 25, no. 5, pp. 1958–1969, 2020.

[15] M. Imani *et al.*, "Voicehd: Hyperdimensional computing for efficient speech recognition," in *ICRC*, pp. 1–8, IEEE, 2017.

[16] P. Poduval *et al.*, "Graphd: Graph-based hyperdimensional memorization for brain-like cognitive learning," *Frontiers in Neuroscience*, p. 5, 2022.

[17] Z. Zou *et al.*, "Scalable edge-based hyperdimensional learning system with brain-like neural adaptation," in *SC*, pp. 1–15, 2021.

[18] A. Hernandez-Cane *et al.*, "Onlinehd: Robust, efficient, and single-pass online learning using hyperdimensional system," in *DATE*, pp. 56–61, IEEE, 2021.

[19] G. Brockman, V. Cheung, L. Pettersson, J. Schneider, J. Schulman, J. Tang, and W. Zaremba, "Openai gym," *arXiv preprint arXiv:1606.01540*, 2016.

[20] T. Chu *et al.*, "Multi-agent deep reinforcement learning for large-scale traffic signal control," *IEEE T-ITS*, vol. 21, no. 3, pp. 1086–1095, 2019.

[21] J. Ke *et al.*, "Optimizing online matching for ride-sourcing services with multi-agent deep reinforcement learning," *arXiv preprint arXiv:1902.06228*, 2019.

[22] H. Ye and G. Y. Li, "Deep reinforcement learning for resource allocation in v2v communications," in *ICC*, pp. 1–6, IEEE, 2018.

[23] S. Wang *et al.*, "Deep reinforcement learning for dynamic multichannel access in wireless networks," *IEEE TCCN*, vol. 4, no. 2, pp. 257–265, 2018.

[24] H.-H. Tseng *et al.*, "Deep reinforcement learning for automated radiation adaptation in lung cancer," *Medical physics*, vol. 44, no. 12, pp. 6690–6705, 2017.

[25] F.-C. Ghesu *et al.*, "Multi-scale deep reinforcement learning for real-time 3d-landmark detection in ct scans," *IEEE TPAMI*, vol. 41, no. 1, pp. 176–189, 2017.

[26] A. Mitrokhin *et al.*, "Learning sensorimotor control with neuromorphic sensors: Toward hyperdimensional active perception," *Science Robotics*, vol. 4, no. 30, 2019.

[27] Y. Kim *et al.*, "Efficient human activity recognition using hyperdimensional computing," in *IOT*, pp. 1–6, 2018.

[28] M. Imani *et al.*, "A framework for collaborative learning in secure high-dimensional space," in *2019 IEEE 12th International Conference on Cloud Computing (CLOUD)*, pp. 435–446, IEEE, 2019.

[29] G. Karunaratne *et al.*, "Robust high-dimensional memory-augmented neural networks," *Nature communications*, vol. 12, no. 1, pp. 1–12, 2021.

[30] M. Imani *et al.*, "Exploring hyperdimensional associative memory," in *HPCA*, pp. 445–456, IEEE, 2017.

[31] R. Bellman, "On the theory of dynamic programming," *Proceedings of the National Academy of Sciences of the United States of America*, vol. 38, no. 8, p. 716, 1952.

[32] H. Hasselt, "Double q-learning," *Advances in neural information processing systems*, vol. 23, pp. 2613–2621, 2010.